Supplementary Information (SI) for Analyst.

Supplementary Section for article entitled "Paper-based Microfluidic Device for Serum Zinc Assay by Colorimetry" by Nath et al. (2024)

1. Design of experiment using Central Composite Design (CCD)

The optimization technique employs the Central Composite Design (CCD) scheme for its general flexibility and acceptance. The response variable (i.e., Euclidean distance) was correlated to five regressor variables, namely (i) buffer pH, (ii) buffer concentration (in M), (iii) dithizone concentration (mM), (iv) dithizone drop volume (μL), and (v) zinc drop volume (μL) (Table S1).

The five parameters CCD scheme led to 2^5 experiments with varied parametric states consisting of 6 central points, 10 axial points, and 16 cube points. Distribution of these points together with the corresponding response are presented in Table S2. We have used Design Expert V.8.0.6 for experiment design.

Table S1. Summary of CCD and levels of the regressor variables for Euclidean distance (as response) in optimization of zinc concentration measurement experiment.

Factor	Name	Units	Coded Values			Mean	SD
			Minimum	Maximum	Alpha (α)		
A	pH of buffer		1.5	7.5	2	4.5	1.3
B	Concentration of buffer	M	4	8		6	0.9
C	Dithizone concentration	mM	0.05	4		2	0.9
D	Dithizone drop volume	μL	0.125	2.625		1.375	0.5
E	Zinc drop volume	μL	2	6		4	0.9

Table S2. Design matrix for the Central Composite Designs (CCD).

Run Order	pH of buffer	Concentration of buffer	Dithizone concentration	Dithizone volume	Zinc drop volume	Euclidian distance
1	6	5	3	0.75	5	0.044
2	6	7	1	2	3	0.035
3	4.5	8	2	1.375	4	0.047

4	4.5	6	0.05	1.375	4	0.051
5	4.5	6	2	1.375	4	0.061
6	6	5	1	2	5	0.027
7	4.5	6	2	0.125	4	0.058
8	4.5	6	2	1.375	4	0.068
9	4.5	4	2	1.375	4	0.035
10	3	7	3	0.75	5	0.044
11	6	7	1	0.75	5	0.041
12	4.5	6	4	1.375	4	0.052
13	6	5	3	2	3	0.039
14	3	5	1	0.75	5	0.035
15	3	5	1	2	3	0.033
16	4.5	6	2	1.375	6	0.047
17	7.5	6	2	1.375	4	0.021
18	4.5	6	2	1.375	4	0.064
19	1.5	6	2	1.375	4	0.023
20	3	5	3	0.75	3	0.028
21	6	5	1	0.75	3	0.044
22	3	5	3	2	5	0.024
23	4.5	6	2	1.375	2	0.044
24	4.5	6	2	1.375	4	0.067
25	4.5	6	2	1.375	4	0.063
26	6	7	3	2	5	0.032

27	3	7	3	2	3	0.044
28	4.5	6	2	1.375	4	0.065
29	3	7	1	0.75	3	0.039
30	6	7	3	0.75	3	0.040
31	4.5	6	2	2.625	4	0.053
32	3	7	1	2	5	0.034

2. Multivariable statistical regression and subsequent parametric optimization:

Different regression models including (i) linear, (ii) 2FI, (iii) quadratic, (iv) cubic were tested (shown in Table S3). We finally, came up with the quadratic model because of high R^2 and ease of use relative to the cubic model. The detailed ANOVA for the quadratic model is presented in Table S4. The F-value was found to be 30.78, which indicates the model to be significant. The probability of the noise significantly impacting the large F-value of the Model is only 0.01%. The "Prob > F" values are less than 0.05, indicating the significance of the terms in the model. The model p-value <0.0001 designates the accuracy of the selected model and also indicates there is very little chance that the system is affected by noise. Additionally, the p-value for the lack of fitness of the model was 0.305 indicating quality validation. Equation S1 represents the final equation in terms of actual parameters.

$$Euclidean\ distance = -0.4258 + 0.058 \times A + 0.079 \times B + 0.004 \times C + 0.032 \times D + 0.044 \times E - 0.002 \times A \times B + 0.0004 \times A \times C - 0.002 \times A \times D - 0.0003 \times A \times E + 0.001 \times B \times C + 0.001 \times B \times D + 0.0004 \times B \times E + 0.0013 \times C \times D + 0.0004 \times C \times E - 0.0047 \times D \times E - 0.005 \times A^2 - 0.006 \times B^2 - 0.004 \times C^2 - 0.006 \times D^2 - 0.005 \times E^2 \quad \text{(S1)}$$

Table S4 also indicates that all coefficients of A, B, C, D, and E (pH of buffer, Concentration of buffer, Dithizone Concentration, Dithizone volume, and Zinc drop volume) were significant.

Table S3. Analysis of different regression models

Source	**Adjusted R-Squared**	**F Value**
Linear	0.13	0.3

2FI	0.71	0.12	
Quadratic	0.95	108.25	**Suggested**
Cubic	0.96	1.62	**Aliased**

Table S4. Analysis of variance (ANOVA) of the chosen quadratic model.

Source	**Sum of Squares**	**Degree of freedom**	**Mean Square**	**F-Value**	**p-value (Prob > F)**
Model	0.0055	20	0.00028	30.78	< 0.0001
A- pH of buffer	1.2×10^{-5}	1	1.2×10^{-5}	1.35	0.27
B-Concentration of buffer	0.00015	1	0.00015	16.23	0.002
C-Dithizone concentration	4.6×10^{-6}	1	4.6×10^{-6}	0.51	0.49
D-Dithizone drop volume	0.00014	1	0.00014	15.15	0.003
E-Zinc drop volume	9.4×10^{-6}	1	9.4×10^{-6}	1.05	0.33
AB	0.00014	1	0.00014	15.45	0.0024
AC	5.06×10^{-6}	1	5.06×10^{-6}	0.57	0.47
AD	3.9×10^{-5}	1	3.9×10^{-5}	4.37	0.06
AE	3.06×10^{-6}	1	3.06×10^{-6}	0.34	0.57
BC	1.4×10^{-5}	1	1.4×10^{-5}	1.57	0.24
BD	5.06×10^{-6}	1	5.06×10^{-6}	0.57	0.47
BE	3.06×10^{-6}	1	3.06×10^{-6}	0.34	0.57
CD	1.06×10^{-5}	1	1.06×10^{-5}	1.18	0.3
CE	3.06×10^{-6}	1	3.06E-06	0.34	0.57
DE	0.00014	1	0.00014	15.45	0.002
A^2	0.0035	1	0.0035	388.9	< 0.0001
B^2	0.0011	1	0.0011	123.47	< 0.0001
C^2	0.0004	1	0.0004	40.89	< 0.0001
D^2	0.0002	1	0.0002	20.63	0.0008
E^2	0.0007	1	0.0007	82.32	< 0.0001
Residual	9.83×10^{-5}	11	8.94×10^{-6}		
Lack of Fit	6.5×10^{-5}	6	1.08×10^{-5}	1.62	0.305
Pure Error	3.33×10^{-5}	5	6.67×10^{-6}		
Cor Total	0.0056	31			

Table S5 shows high R^2 as well as closeness among R^2, adjusted R^2, and predicted R^2. The results confirmed a good parity, high precision, and presence of significant terms only in the model equation. Therefore, the model is able to accurately predict the Euclidean distance for any zinc concentration.

Table S5. Statistical parameters obtained by ANOVA for the model proposed.

R^2	Adj. R^2	Pred. R^2	SD
0.98	0.95	0.92	0.0029

Figure S1 shows the contour plots of the response surface demonstrating comparable influences of all five parameters (i.e., pH of buffer, buffer concentration, Dithizone concentration, Dithizone drop volume, Zinc drop volume).

(a)

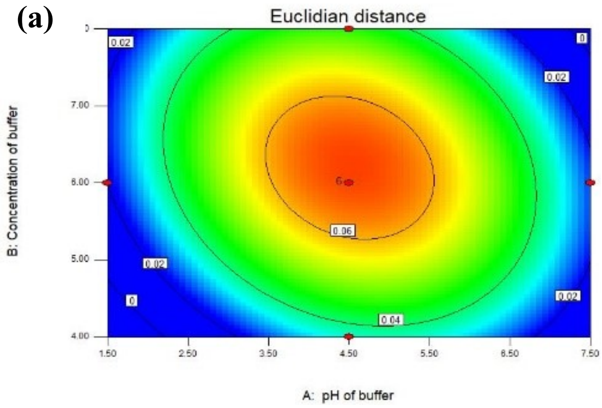

(b)

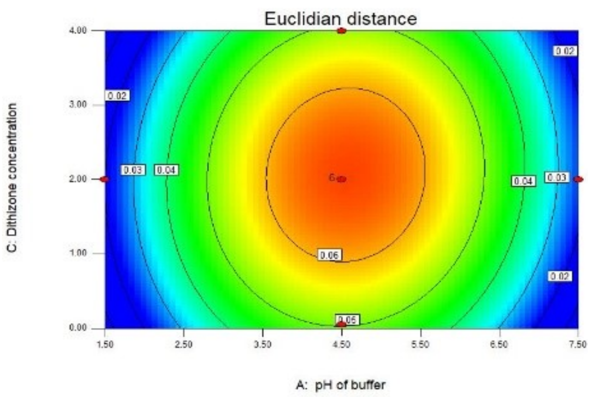

(c)

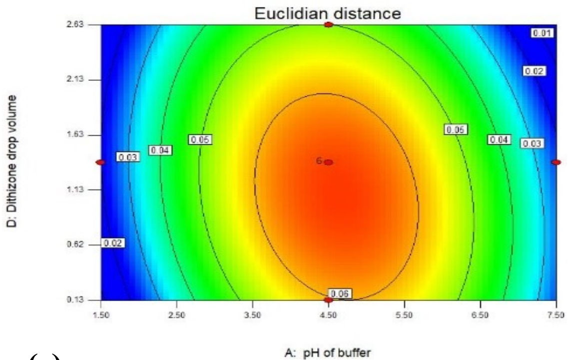

(d)

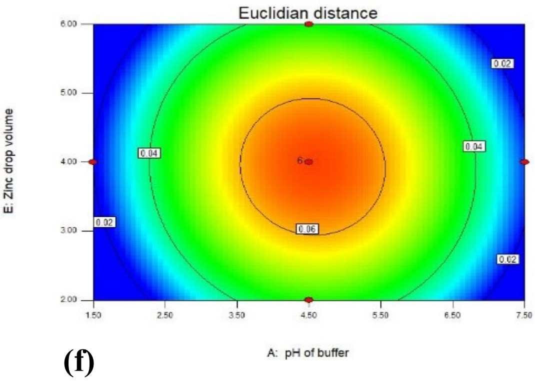

(e)

(f)

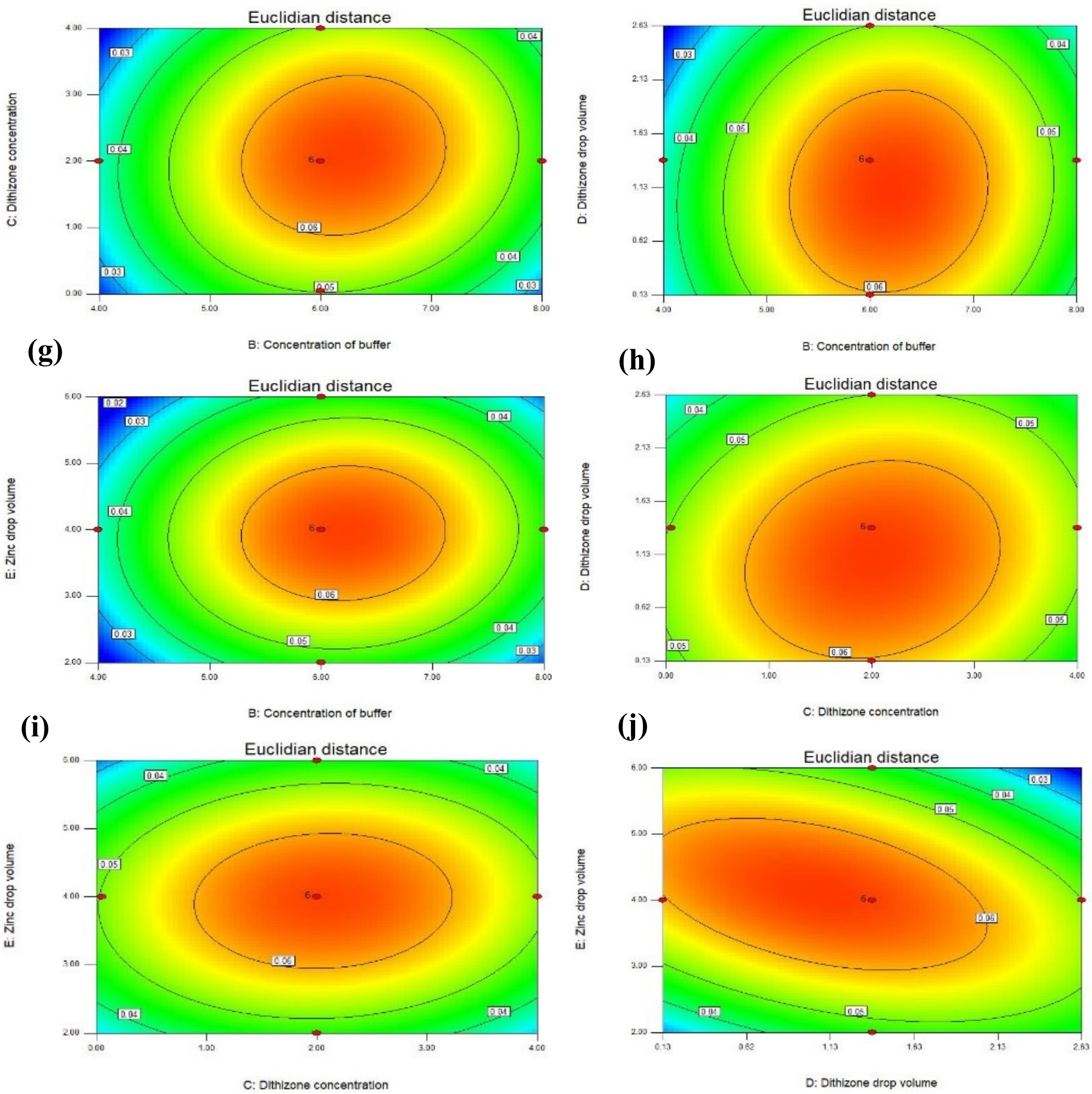

Figure S1. Contour plots representing the variations of Euclidian distance as a function of (a) pH of buffer and concentration of buffer, (b) pH of buffer and concentration of dithizone, (c) pH of buffer and volume of dithizone drop, (d) pH of buffer and volume of zinc drop, (e) concentration of dithizone and concentration of buffer (f) volume of dithizone drop and concentration of buffer (g) volume of zinc drop and concentration of buffer (h) volume of dithizone drop and concentration of dithizone (i) volume of zinc drop and concentration of dithizone (j) volume of zinc drop and volume of dithizone drop. (Each of the contour plots are formed between two variables while 3 other variables are kept constant at optimized value)

(1) Effect of pH of buffer:

The interactions of buffer pH with the other regressor variables were quite significant. Colour intensity was highest at the pH range of 3.5-5.6 and the range for other design parameters are as follow: buffer concentration range of 5.3-7.1 M, dithizone concentration range of 0.9-3.2 mM, dithizone volume range of 0.1-2 µL, and lastly, zinc drop volume range of 2.9-4.9 µL (Figure S1 (a)-(d)). We can see that the pH is optimized at 4.5 through theoretical model obtained by statistical analysis. This may be because at pH 4.5 (mild acidic medium) the stability of zinc dithizonate complex is highest and the interference of other ions is minimal.

Catapeno et al.[1] have confirmed the maximum absorbance at pH 4.5 for both instantaneous measurement and that 5 min after the reaction in zinc chelation using dithizone. Moreover, Fischer et al.[2] also demonstrated the need for weakly acidic medium for zinc detection. Imperatively, in acetate buffer at pH 4.5, the decomposition of zinc dithizonate is noted to be extremely slow. Thus, the coloured zinc dithizonate complexes is more stable and colour intensity became maximum. As referred by Margerum et al.[3] when zinc is to be kept noninteracting with cadmium and lead in a solution, it is recommended to maintain a pH 4.5 for effective separation of zinc[4] from the other interfering ions. Irving et al.[5] demonstrated zinc leaching from soil by setting buffer acetate solution with pH 4.5 by dithizone in chloroform system. Li et al.[6] have also performed detection of zinc in water sample from various sources using μPAD. There also they have used acetate buffer of pH 4.5 to detect zinc efficiently.

(2) Effect of concentration of buffer:

The effect of concentration of buffer on the color intensity and also its variation with other factors is depicted by the contour plots (Figure S1 (a), (e)-(g)). It was observed that the color intensity was highest over the buffer concentration range 5.3-7.1 M and the range of other design parameters were similar, as before. We could observe the optimized value of concentration to be 6 M. With increase in the concentration above 6 M, the Euclidean distance remains maximum till 7.1 M, beyond it starts decreasing. This may be because at low concentration of buffer, enough molecules of sodium acetate and acetic acid are not present to stabilize the pH at 4.5 and thus, the other metal ions interfere with zinc and do not let zinc react with dithizone and also the zinc dithizonate complex is not stable. Previous reports also suggest to maintain the acetate buffer concentration for metal ion detection at 6.3. M. Li et al.[6] also performed the detection of zinc in μPAD and used an acetate buffer of 6.3 M to maintain the pH of the system at 4.5. Tan et al.[7] demonstrated detection of copper using acetate buffer of 6.3 M. Hence, we have used acetate buffer concentration of 6.3 M in the present analysis.

(3) Effect of dithizone concentration:

From the contour plots (Figure S1 (b), (e), (h), and (i)), we can see the optimum value of dithizone concentration is obtained at 2 mM. If the dithizone concentration is low then the stoichiometric demand (zinc: dithizone= 1:2) of the reaction will not be fulfilled. Dithizone, when mixed in chloroform produces a characteristic green hue. Thus, if the concentration of dithizone is too high, the color of dithizone spot will be so saturated that when zinc is added, it would be impossible to detect minute colour change. Hence, it is required to maintain sufficient quantity of indicator for zinc detection. Li et al.[6] and Grabaric et al.[8] have also used 1.95 mM dithizone to detect metal ions having the same stoichiometric ratio as zinc-dithizone reaction. Thus, in our investigation, we used 1.95 mM dithizone as the colorimetric reagent for zinc detection.

(4) Effect of dithizone drop volume:

From the contour plots (Figure S1 (c), (f), (h), and (j)), we can clearly visualize the dithizone drop volume to be spotted on the reaction zone is achieving its optima at 1.375 µL. We have used 1 µL in our experiments. We optimized the reagent volume in such a way that its volume could be kept minimum to reduce the cost. However, the reagent molecules per drop available on the reaction zone should also be sufficient to react with the available zinc. As the concentration of reagent was kept high, we used a reduced droplet size of the reagent.

(5) Effect of zinc drop volume:

Contour plots clearly indicate (Figure S1 (d), (g), (i), and (j)) the optimized zinc droplet volume to be 4 µL. The highest zinc concentration to be detected in the current experiment was 25 µM. The Dithizone concentration used here is 1.95 mM and dithizone drop volume was optimized at 1 µL. Thus, we can get a ratio of zinc to dithizone moles to be 1:20. That means the dithizone is almost 10 times more than the stoichiometric requirement. Catapeno et al.[1], suggested to use a dithizone concentration > 3 times than the highest zinc concentration. Thus, in order to keep dithizone molecules in slight excess to zinc, we considered the optimized value at 4 µL.

3. Gold standard method (by AAS) of serum zinc assay

In AAS, a hollow cathode lamp (HCl lamp of zinc) was used emitting a monochromatic light of wavelength 213.9 nm, which corresponds to the maximum absorbance of zinc. The AAS was operated in flame mode with oxyacetylene flame (Acetylene pressure: 0.8 kg/cm^2, Air pressure: 4 kg/cm^2, Acetylene flow: 2.5 L/min, Air flow: 10 L/min) burned at 2400 °C. The light passed through a slit of 0.7 nm. Instrument was calibrated using standard solutions of zinc of the following concentrations 7.65 µM (absorbance: 0.195), 15.30 µM (absorbance: 0.379), and 38.24 µM (absorbance: 0.742), respectively. The serum samples were diluted with millipore water at 1:1 by volume. Then, based on the calibration curve, we can get absorbance of the unknown serum samples and their corresponding concentrations.

4. Design specifications of µ-PAD

To finalize the µPAD design, we had systematically explored the performance-wise variations of different spotting wells and channels with varied dimensions. Two design variants were majorly explored in need for the uniformity in colour distribution. Remarkably, an observable correlation emerged wherein the imbibition of the solutions exhibited a decelerating trend concurrent with an increase in both channel width and length. This phenomenon is posited to arise from increased paper resistance, potentially instigating a gradual evaporation process. Also, the presence of carboxyl group on paper fibres leads to the formation of negative surface charge that interacts with positively charged metal ions by spontaneous and reversible sorption. Adsorption of Zn^{2+} ions from analyte on paper may lead to lowering the number of ions reaching the detection zone to bond with dithizone and thereby, resulted in reduced colour intensity[9]. Thus, we concluded that the spotting wells were simpler to operate and produced relatively distinct images compared to channels. We selected spotting well with hydrophobic wall instead of simple unbounded spotting regions because the hydrophobic wall restricts the zinc drop within the detection zone to avoid the loss of intensity due to loss of zinc upon indefinite spread. The circular sampling zone was used to facilitate uniform spreading of the droplet through the internal area. The droplet volume of the reagent and analyte were optimized at a ratio of 1:4. The reagent dissolved in chloroform was not restricted by the hydrophobic barrier. Thus, the reagent zone should have a diameter so that the drop of dithizone in chloroform should not be crossing the hydrophobic boundary. On the other hand, increasing the zone diameter evidently led to the increase in reagent and sample volumes. Such increase of total volume increases the moisture content on the paper surface, which in turn hinder proper imaging for analysis and also the formation of metal chelates. Thus, determining the optimum spotting well diameter was quite important. Thus, through repeated trial and error, we finalized the spotting zone of 7 mm diameter bounded by a 1 mm hydrophobic barrier. The Figure S2 depicts the proposed µPAD.

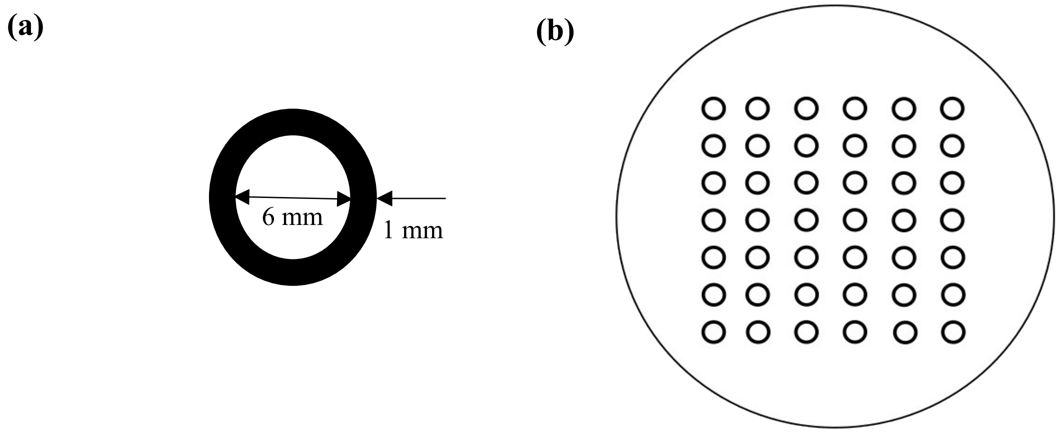

Figure S2. (a) Optimized dimension of individual spotting wells (b) 7 × 6 array of spotting wells printed on a single filter paper.

5. *Statistical analysis for selection of solvents and maximum colour intensity for detection module*

   Calibration plots in terms of absolute intensity measures versus zinc concentration for two selected solvents (chloroform and ethanol) are presented in Figure S3. Table S6 provides the statistical test parameters of the calibration plots in terms of normalized intensities.

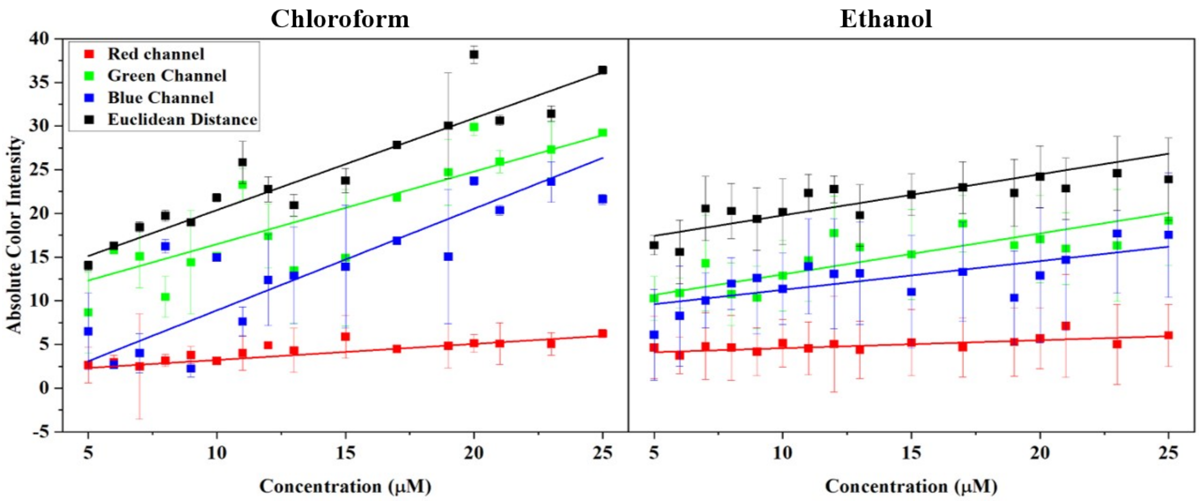

Intensity measures	Coefficient of linearity (R^2)		Mean standard deviation (mean SD)		Mean square error (MSE)		Intraclass Correlation Coefficient (ICC)	
Solvent	**Chloroform**	**Ethanol**	**Chloroform**	**Ethanol**	**Chloroform**	**Ethanol**	**Chloroform**	**Ethanol**
ΔR	0.920	0.546	21.4	16.8	13.73	13.27	0.31	0.055
ΔG	0.922	0.735	24.9	31.7	22.36	46.76	0.29	0.03
ΔB	0.88	0.485	27.8	32.9	24.37	49.88	0.33	0.048
ΔE	0.952	0.727	16.03	41.6	9.18	73.46	0.76	0.08

Figure S3. Calibration plots for absolute intensity measures. The table represents different statistical test parameters for absolute intensity measures.

Table S6. Statistical test parameters related to the calibration plots for normalized intensities.

Intensity measures	Coefficient of linearity (R^2)		Mean standard deviation (mean SD)		Mean square error (MSE)		Intraclass Correlation Coefficient (ICC)	
Solvent	**Chloroform**	**Ethanol**	**Chloroform**	**Ethanol**	**Chloroform**	**Ethanol**	**Chloroform**	**Ethanol**
$\frac{\Delta R}{R}$	0.921	0.804	0.17	0.11	7×10^{-4}	6×10^{-4}	0.55	12×10^{-4}
$\frac{\Delta G}{G}$	0.811	0.925	0.27	0.22	16×10^{-4}	25×10^{-4}	0.44	0.027
$\frac{\Delta B}{B}$	0.937	0.766	0.23	0.21	11×10^{-4}	22×10^{-4}	0.54	0.012
$\frac{\Delta E}{E}$	0.939	0.851	0.17	0.16	6×10^{-4}	14×10^{-4}	0.96	0.47

6. Parity diagram of zinc in aqueous solution.

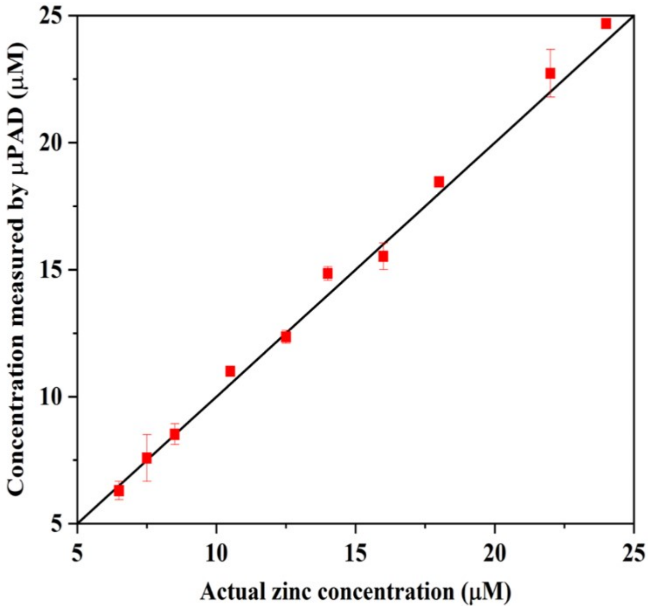

Figure S4. Parity diagram showing the closeness of measured and actual zinc concentration in aqueous solution.

7. Experimental validation of present technique with respect to AAS-based measurements

Table S7. Comparative analysis of present method with the results based on AAS.

	Sl. No	Sample Type	Values from AAS	Current Method	Diagnosis	Truth table
ZINC DEFICIENT	1	Diseased	4.1	3.8	Diseased	TP
	2	Diseased	5.2	5.3	Diseased	TP

3	Diseased	5.7	5.2	Diseased	TP
4	Diseased	6.1	5.8	Diseased	TP
5	Diseased	6.2	5.7	Diseased	TP
6	Diseased	6.2	7.6	Diseased	TP
7	Diseased	6.3	6.3	Diseased	TP
8	Diseased	6.4	6.7	Diseased	TP
9	Diseased	6.4	5.5	Diseased	TP
10	Diseased	6.5	6.5	Diseased	TP
11	Diseased	6.6	6.6	Diseased	TP
12	Diseased	6.7	7.6	Diseased	TP
13	Diseased	6.8	6.8	Diseased	TP
14	Diseased	6.9	6.5	Diseased	TP
15	Diseased	6.9	5.52	Diseased	TP
16	Diseased	7.0	7.1	Diseased	TP
17	Diseased	7.0	7.1	Diseased	TP
18	Diseased	7.1	6.0	Diseased	TP
19	Diseased	7.2	7.2	Diseased	TP
20	Diseased	7.3	7.6	Diseased	TP
21	Diseased	7.3	7.4	Diseased	TP
22	Diseased	7.4	7.2	Diseased	TP
23	Diseased	7.5	7.6	Diseased	TP
24	Diseased	7.5	8.2	Diseased	TP
25	Diseased	7.5	7.6	Diseased	TP

	26	Diseased	7.5	7.2	Diseased	TP
	27	Diseased	7.8	8.0	Diseased	TP
	28	Diseased	8.0	9.1	Diseased	TP
	29	Diseased	8.1	8.2	Diseased	TP
	30	Diseased	8.1	8.3	Diseased	TP
	31	Diseased	8.2	8.4	Diseased	TP
	32	Diseased	8.2	8.4	Diseased	TP
	33	Diseased	8.3	8.5	Diseased	TP
	34	Diseased	8.3	8.5	Diseased	TP
	35	Diseased	8.4	8.6	Diseased	TP
	36	Diseased	8.4	8.7	Diseased	TP
HEALTHY	37	Diseased	8.6	8.8	Diseased	TP
	38	Diseased	8.7	8.9	Diseased	TP
	39	Diseased	8.7	8.9	Diseased	TP
	40	Diseased	8.7	9.0	Diseased	TP
	41	Diseased	8.8	9.2	Healthy	FN
	42	Diseased	8.9	9.2	Healthy	FN
	43	Healthy	9.2	8.5	Diseased	FP
	44	Healthy	9.2	9.1	Diseased	FP
	45	Healthy	9.2	9.5	Healthy	TN
	46	Healthy	9.2	9.5	Healthy	TN
	47	Healthy	9.3	9.6	Healthy	TN
	48	Healthy	9.3	9.1	Diseased	FP

49	Healthy	9.3	8	Diseased	FP
50	Healthy	9.3	9.7	Healthy	TN
51	Healthy	9.8	10.2	Healthy	TN
52	Healthy	9.9	10.3	Healthy	TN
53	Healthy	9.9	10.3	Healthy	TN
54	Healthy	10.3	10.7	Healthy	TN
55	Healthy	10.4	10.7	Healthy	TN
56	Healthy	11.4	11.9	Healthy	TN
57	Healthy	11.8	12.5	Healthy	TN
58	Healthy	13.9	12.6	Healthy	TN
59	Healthy	14.7	15.5	Healthy	TN

8. *Recovery and Precision dataset and calculations*

1_1 = Sample_spiked (5 μM)

1_1_0 = Sample_uspiked

2_1 = Sample_spiked (10 μM)

2_1_0 = Sample_uspiked

3_1 = Sample_spiked (15 μM)

3_1_0 = Sample_uspiked

5, 10, 15 μM concentration of artificial plasma added to real sample of concentration 9.76 μM

Average concentration from calibration plot = $\frac{Average\ Intensity\ Experimental - 0.0069}{0.0076}$ (S2)

a) Recovery:

i. Intraday

Table S8. Table of Recovery (Intraday) calculations.

Sample no	$\Delta E_W/E_W$	$Average$ $\Delta E_W/E_W$	$Average$ $Unspiked$ $\Delta E_W/E_W$	Average concentration from calibration plot	Concentration added (Cadd)	%Recovery	Intraday %Recovery
1_1	0.1197			14.84	5	101.28	94.73
	0.1177			14.58		95.94	
	0.1143			14.13		86.98	
2_1	0.1499			18.82	10	90.45	92.89
	0.156			19.58		98.05	
	0.139			17.42		76.45	
	0.1623			20.44		106.63	
3_1	0.183			23.22	15	89.59	97.34
	0.204			25.98		108	
	0.189			23.95		94.44	
1_1_0	0.082	0.0814	0.0812	9.78			
	0.087						
	0.075						
2_1_0	0.0866	0.082					
	0.0834						
	0.076						
3_1_0	0.088	0.0802					
	0.072						
	0.08						

ii. Interday

Table S9. Table of Recovery (Interday) calculations.

Sample No	Concentration (µM)	R_b	G_b	B_b	R	G	B	$\Delta E_W/E_W$	$Average$ $\Delta E_W/E_W$	$Average$ $Unspiked$ $\Delta E_W/E_W$	Average concentration from calibration plot	Concentration added (Cadd)	%Recovery	Interday %Recovery
1_1	14.27	171.2	160.7	172.6	157.92	148.01	142.95	0.1197	0.1172		14.52	5	94.73	84.39
		171.2	160.7	172.6	160.26	140.56	147.07	0.1177						
		171.2	160.7	172.6	158.65	143.29	147.14	0.1143						
1_1_0	9.76	171.2	160.7	172.6	163.04	145.16	156.41	0.082	0.0814	0.0812	9.78			
		171.2	160.7	172.6	161.62	151.69	150.79	0.087						
		171.2	160.7	172.6	161.88	142.36	165.18	0.075						
1_1	14.27	171.2	160.7	172.6	163.87	147.2	153.52	0.0991	0.1112		13.72	5	78.54	
		171.2	160.7	172.6	165.05	145.42	147.28	0.115						
		171.2	160.7	172.6	163.75	149.81	143.3	0.1197						
1_1_0	9.76	171.2	160.7	172.6	170.83	145.6	151.78	0.097	0.081	0.0813	9.795			
		171.2	160.7	172.6	173.77	157.99	152.71	0.07						
		171.2	160.7	172.6	173.65	156.84	151.61	0.0751						
1_1	14.27	171.2	160.7	172.6	178.4	144.94	143.08	0.1096	0.112		13.78	5	79.91	
		171.2	160.7	172.6	177.26	143.34	140.69	0.119						

2_1_0			2_1			2_1_0			2_1			1_1_0			
9.76			19.27			9.76			19.27			9.76			
171.2	171.2	171.2	171.2	171.2	171.2	171.2	171.2	171.2	171.2	171.2	171.2	171.2	171.2	171.2	171.2
160.7	160.7	160.7	160.7	160.7	160.7	160.7	160.7	160.7	160.7	160.7	160.7	160.7	160.7	160.7	160.7
172.6	172.6	172.6	172.6	172.6	172.6	172.6	172.6	172.6	172.6	172.6	172.6	172.6	172.6	172.6	172.6
165.28	169.73	171.08	159.35	155.17	153.83	162.24	162.02	161.68	144.08	165.24	165.21	164.33	170.29	169.72	168.00
157.94	157.74	156.58	149.1	142.54	138.26	152.9	148.85	152.89	114.18	138.41	134.38	145.96	146.74	148.18	142.38
150.56	155.10	147.61	142	144.28	136.14	153.92	153.47	150.58	112.26	139.18	130.07	156.57	154.01	151.18	147.22
0.088	0.068	0.0899	0.131	0.143	0.17	0.076	0.0834	0.0866	0.2775	0.139	0.173	0.082	0.0781	0.083	0.1063
0.0819			0.149			0.082			0.156			0.081			
0.0813						0.0812						0.0813			
9.795			18.63			9.78			19.62			9.79			
			10						10						
			88.4						98.38						
									89.47						

3_1			**3_1_0**			**3_1**			**2_1_0**			**2_1**		
	24.27			9.76			24.27			9.76			19.27	
171.2	171.2	171.2	171.2	171.2	171.2	171.2	171.2	171.2	171.2	171.2	171.2	171.2	171.2	171.2
160.7	160.7	160.7	160.7	160.7	160.7	160.7	160.7	160.7	160.7	160.7	160.7	160.7	160.7	160.7
172.6	172.6	172.6	172.6	172.6	172.6	172.6	172.6	172.6	172.6	172.6	172.6	172.6	172.6	172.6
164.68	147.18	159.81	165.15	162.52	165	144.12	145.15	149.88	191.39	183.27	187.86	161.87	152.9	154.32
144	132.74	131.19	147.59	151.1	155.73	135.1	125.6	133.3	144.25	154.64	149.85	142.56	141.5	143
136.92	138.93	139.27	154.27	155.93	148.14	132.1	132.17	131.98	159.12	147.87	156	137.34	140.65	138.37
0.145	0.187	0.1697	0.08	0.072	0.088	0.189	0.204	0.183	0.089	0.084	0.076	0.139	0.145	0.1461
	0.167			0.0802			0.192			0.083			0.143	
				0.0812						0.0813				
	21.095			9.78			24.38			9.79			17.95	
	15						15						10	
	75.33						97.34						81.63	
							87.78							

3_1_0			**3_1**			**3_1_0**		
9.76			24.27			9.76		
171.2	171.2	171.2	171.2	171.2	171.2	171.2	171.2	171.2
160.7	160.7	160.7	160.7	160.7	160.7	160.7	160.7	160.7
172.6	172.6	172.6	172.6	172.6	172.6	172.6	172.6	172.6
174.61	171.84	175.42	159.46	161.2	155.77	164.59	165.76	161.57
149.96	145.09	149.37	128.08	130.31	128.41	156.19	163.5	161.6
147.46	155.9	151.85	136.95	124.35	131.95	154.51	149.87	157.48
0.0878	0.077	0.076	0.17	0.196	0.186	0.081	0.086	0.0766
0.0801			0.185			0.081		
0.0813						0.0813		
9.79			23.39			9.795		
			15					
			90.67					

b) Precision:

i. Intraday

Table S10. Table of Precision (Intraday) calculations.

Sample no	Concentration (µM)	%Recovery	Mean value	Standard Deviation	Intraday Precision or %Relative Standard Deviation
1_1	14.27	101.28	94.73	7.23	7.63
		95.94			
		86.98			
2_1	19.27	90.45	92.89	12.8	13.78
		98.05			
		76.45			
		106.63			

3_1	24.27	89.58 108 94.44	97.34	9.55	9.81
1_1_0	9.76				
2_1_0	9.76				
3_1_0	9.76				

ii. Interday

Table S 11. Table of Precision (Interday) calculations.

Sample No	Concentration (µM)	%Recovery	Mean value	Standard Deviation	Interday Precision or %Relative Standard Deviation
1_1	14.27	94.73	84.39	8.98	10.64
1_1_0	9.76				
1_1	14.27	78.54			
1_1_0	9.76				
1_1	14.27	79.91			
1_1_0	9.76				
2_1	19.27	98.38	89.47	8.43	9.42
2_1_0	9.76				
2_1	19.27	88.4			
2_1_0	9.76				
2_1	19.27	81.63			
2_1_0	9.76				
3_1	24.27	97.34	87.78	11.29	12.86
3_1_0	9.76				
3_1	24.27	75.33			
3_1_0	9.76				
3_1	24.27	90.67			
3_1_0	9.76				

9. *Rapid zinc detection application detailed methodology and comparison with ImageJ*

Link to the published application algorithm: https://github.com/knath28/knath28-Zinc-concentration-application

(a)

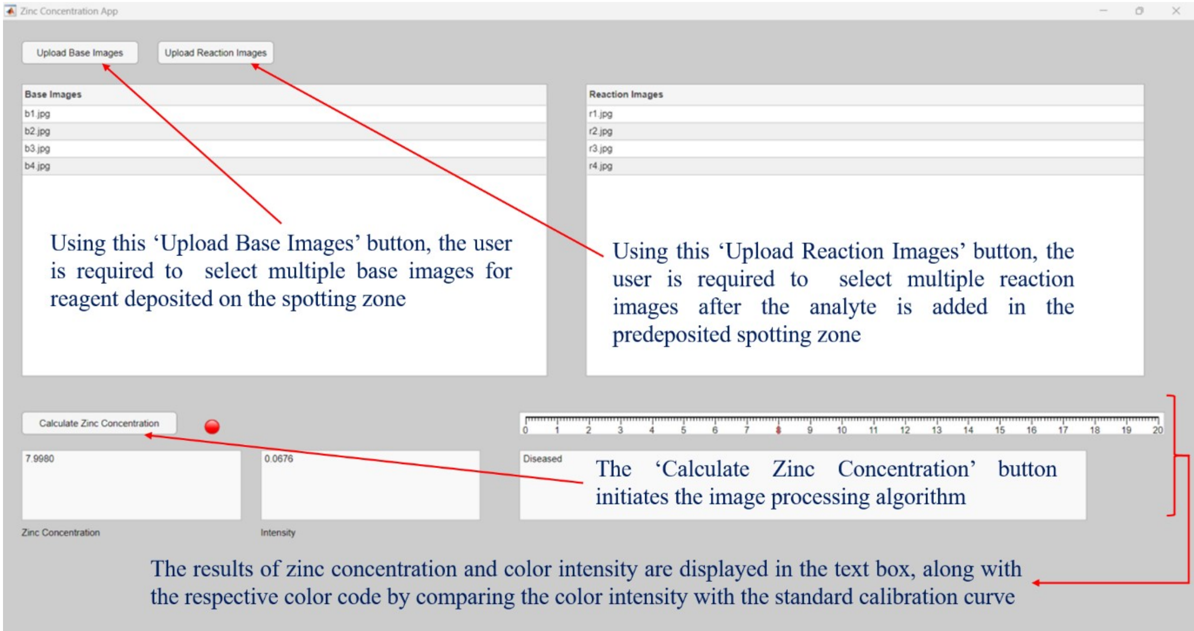
Zinc Concentration App
Upload Base Images
Upload Reaction Images
Base Images
b1.jpg
b2.jpg
b3.jpg
b4.jpg
Reaction Images
r1.jpg
r2.jpg
r3.jpg
r4.jpg
Using this 'Upload Base Images' button, the user is required to select multiple base images for reagent deposited on the spotting zone
Using this 'Upload Reaction Images' button, the user is required to select multiple reaction images after the analyte is added in the predeposited spotting zone
Calculate Zinc Concentration
0 1 2 3 4 5 6 7 8 9 10 11 12 13 14 15 16 17 18 19 20
7.9980
0.0676
Diseased
The 'Calculate Zinc Concentration' button initiates the image processing algorithm
Zinc Concentration
Intensity
The results of zinc concentration and color intensity are displayed in the text box, along with the respective color code by comparing the color intensity with the standard calibration curve

(b)

(c)

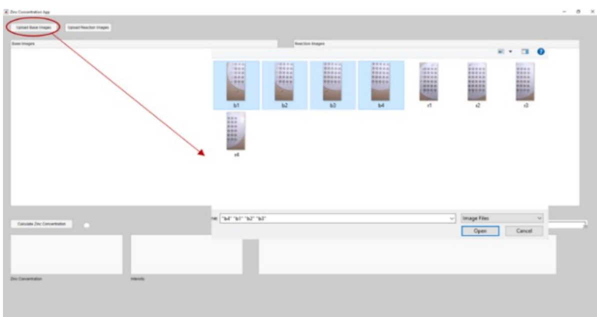

(d)

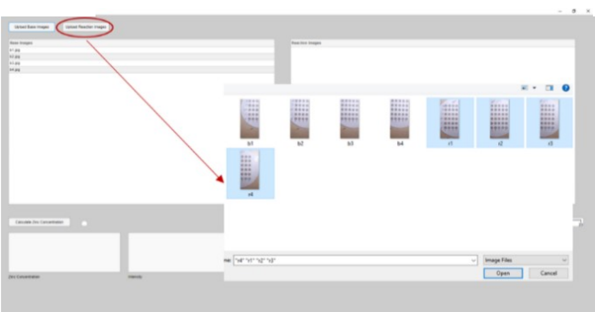

(e)

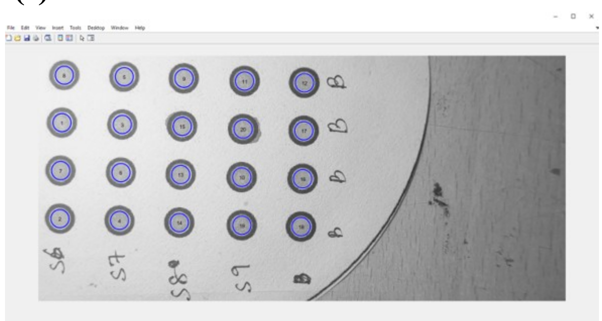

(f)

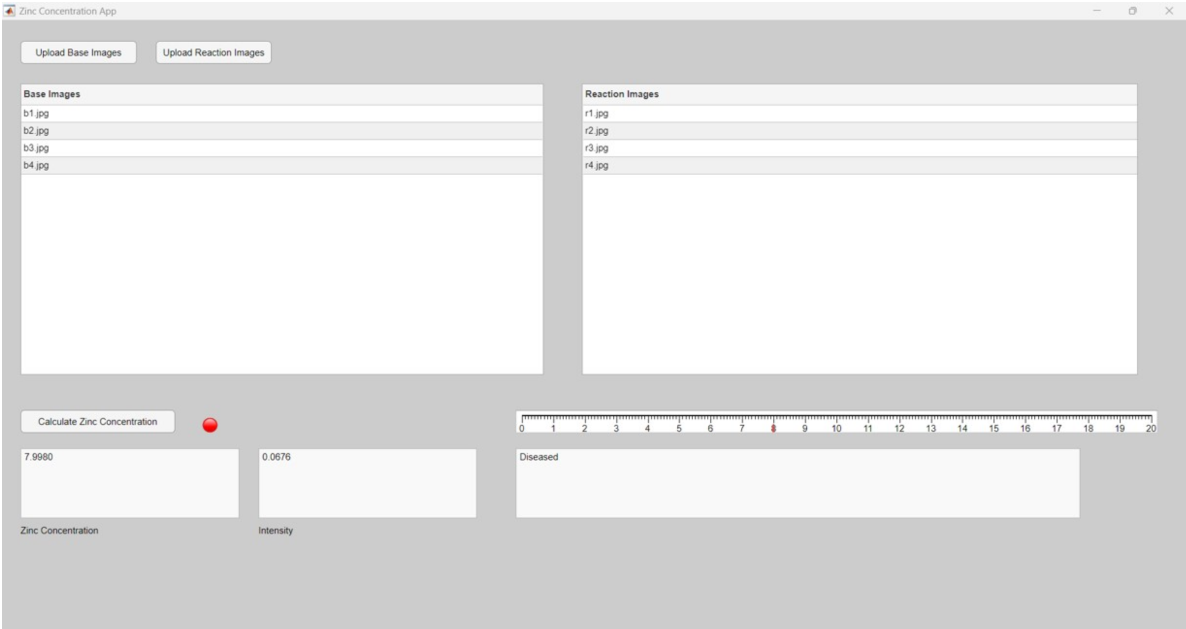

Figure S5. (a) Schematic of the steps to analyse images in graphical user interface of the MATLAB-based application (IZD), (b) Initial user interface, (c) Uploading multiple base images after reagent deposition, (d) Uploading multiple reaction zone images after spotting of analyte (e) Selecting the region of interest in the images selected by user (f) Final result window.

Table S12. Comparison between the image color intensities between ImageJ and IZD (Instant Zinc Detection) application.

$$\%\,Relative\ Error = \frac{Colour\ intensity\ (ImageJ) - Colour\ intensity\ \ (App.)}{Colour\ intensity\ \ (ImageJ)} \times 100\%$$

(S3)

Sl. No.	Colour intensity obtained from the App.	Colour intensity obtained from ImageJ	Category based on zinc concentration	% Relative Error	Average % Relative Error
1	0.050	0.050	Diseased	0	1.91
2	0.050	0.050	Diseased	0	
3	0.048	0.048	Diseased	0	
4	0.057	0.055	Diseased	3.63	
5	0.056	0.054	Diseased	3.7	

6	0.061	0.062	Diseased	1.61
7	0.064	0.067	Diseased	4.48
8	0.068	0.070	Diseased	2.86
9	0.070	0.071	Diseased	1.41
10	0.071	0.070	Diseased	1.43
11	0.070	0.071	Diseased	1.41
12	0.073	0.073	Diseased	0
13	0.077	0.079	Diseased	2.53
14	0.076	0.074	Diseased	2.7
15	0.100	0.104	Diseased	3.85
16	0.125	0.120	Diseased	4.17
17	0.062	0.062	Diseased	0
18	0.064	0.063	Diseased	1.59
19	0.072	0.070	Diseased	2.86
20	0.056	0.056	Diseased	0
21	0.0767	0.075	Diseased	2.27
22	0.070	0.070	Diseased	0
23	0.064	0.064	Diseased	0
24	0.085	0.084	Diseased	1.19
25	0.046	0.049	Diseased	6.12
26	0.076	0.072	Diseased	5.56
27	0.075	0.077	Diseased	2.59
28	0.065	0.066	Diseased	1.5

29	0.064	0.065	Diseased	1.54
30	0.076	0.077	Diseased	1.29
31	0.075	0.074	Diseased	1.35
32	0.058	0.055	Diseased	5.45
33	0.075	0.069	Diseased	8.69
34	0.047	0.049	Diseased	4.09
35	0.069	0.07	Diseased	1.43
36	0.062	0.06	Diseased	3.33
37	0.061	0.061	Diseased	0
38	0.060	0.060	Diseased	0
39	0.051	0.050	Diseased	2
40	0.052	0.051	Diseased	1.96
41	0.063	0.061	Healthy	3.28
42	0.059	0.059	Healthy	0
43	0.035	0.036	Diseased	2.78
44	0.049	0.047	Diseased	4.26
45	0.085	0.083	Healthy	2.41
46	0.074	0.074	Healthy	0
47	0.074	0.073	Healthy	1.37
48	0.088	0.084	Diseased	4.76
49	0.079	0.081	Diseased	2.47
50	0.072	0.072	Healthy	0
51	0.067	0.068	Healthy	1.47

52	0.071	0.071	Healthy	0
53	0.103	0.103	Healthy	0
54	0.088	0.089	Healthy	1.12
55	0.080	0.080	Healthy	0
56	0.084	0.084	Healthy	0
57	0.079	0.079	Healthy	0
58	0.079	0.079	Healthy	0
59	0.097	0.097	Healthy	0

References

(1) Catapano, M. C.; Tvrdý, V.; Karlíčková, J.; Mercolini, L.; Mladěnka, P. A Simple, Cheap but Reliable Method for Evaluation of Zinc Chelating Properties. Bioorg Chem **2018**, 77, 287–292. https://doi.org/10.1016/J.BIOORG.2018.01.015.

(2) Fischer Hellmut; Leopoldi Grete. Detection and Determination of Small Amounts of Zinc with Dithizone. Ztschrft. f. anal. Chem. **1936**, 107, 241–269. https://doi.org/10.1007/BF01391595.

(3) Margerum, D. W.; Santacana1, F. Evaluation of Methods for Trace Zinc Determination. Anal Chem **1960**, 32 (9), 1157–1161. https://doi.org/10.1021/ac60165a032.

(4) Sylvester, N. D.; Hughes, E. B. The Determination of Zinc in Foods. Analyst **1936**, 61, 734–742. https://doi.org/10.1039/AN9366100734.

(5) Irving, H. M. N. H. The Analytical Applications Of Dithizone. C R C Critical Reviews in Analytical Chemistry **1980**, 8 (4), 321–366. https://doi.org/10.1080/10408348008542714.

(6) Li, F.; Hu, Y.; Li, Z.; Liu, J.; Guo, L.; He, J. Three-Dimensional Microfluidic Paper-Based Device for Multiplexed Colorimetric Detection of Six Metal Ions Combined with Use of a Smartphone. Anal Bioanal Chem **2019**, 411 (24), 6497–6508. https://doi.org/10.1007/s00216-019-02032-5.

(7) Tan, W.; Zhang, L.; Shen, W. Low-Cost Chemical-Responsive Adhesive Sensing Chips. ACS Appl Mater Interfaces **2017**, 9 (48), 42366–42371. https://doi.org/10.1021/acsami.7b14122.

(8) Et, G. Improved Signals Ratio Resolution Method by Optimization of Resolution Function-Simultaneous Determination of Cu(II) and Cd(II) in Water Samples. J AOAC Int **1999**, 82 (5), 1185–1197. https://doi.org/10.1093/jaoac/82.5.1185.

(9) Lewińska, I.; Ścibisz, M.; Tymecki, Ł. Microfluidic Paper-Based Analytical Device for Simultaneous Determination of Calcium and Magnesium Ions in Human Serum. Anal Chim Acta **2024**, 1308. https://doi.org/10.1016/j.aca.2024.342639.